Re-entry and Flight Dynamics of a Winged Reusable First Stage

Sven Stappert, Steffen Callsen* and Dr. Martin Sippel**
**German Aerospace Center (DLR), Robert-Hooke-Straße 7, 28359 Bremen*

Abstract

Reusing launch vehicle stages has the potential to reduce launch costs and is hence of high interest in the context of defining the next generation of European launch vehicles. Winged reusable first stages have been a focus of the system launcher analysis group at DLR in the past years. Using wings and other aerodynamic surfaces, the aerodynamic forces during re-entry are used to safely decelerate the vehicle, thus rendering the reignition of any engines and the use of propellants unnecessary. Nevertheless, the design of a winged first rocket stage capable of fulfilling its main objective, accelerating the launch vehicle from ground up to stage separation, while also being able to do an autonomous and controlled atmospheric re-entry offers its challenges. Traversing from hypersonic to subsonic velocities, the vehicle has to be controllable at a vast range of flight conditions. Understanding the flight dynamics behind the re-entry of a winged vehicle in an early design stage is necessary to identify challenges with regards to controlling and actively steering such a high-performance vehicle in order arrive at a feasible and robust design that does not fail to converge in later design iterations. This work focuses on the analysis of the vehicle dynamics using linearized dynamic equations with 6 degrees of freedom. The controllability using aerodynamic surfaces and RCS shall be investigated and, possibly, proven by simulation.

AoA	Angle of Attack	GTO	Geostationary Transfer Orbit
CoG	Center of Gravity	RCS	Reaction Control System
DOF	Degrees of Freedom	RLV	Reusable Launch Vehicle
ELV	Expendable Launch Vehicle		
FPA	Flight Path Angle		

1. Introduction

In the past years the idea of reusing launch vehicles, or parts of launch vehicles, has gained in popularity again, partly thanks to the success of SpaceX in frequently landing and reusing the Falcon 9 first stage. Since then SpaceX has advanced to a major player and competitor in space transportation, challenging Europe to come up with innovative ideas to keep up with the recent developments. Hence for a future generation of potentially reusable European launch vehicles it is of crucial importance to understand the implications of reusability on the launch system and to identify technical challenges, advantages and drawbacks of different recovery methods..

Different pathways of achieving reusability in launch vehicle design have been studied in the past and present at DLR [1], [2]. Whereas SpaceX focuses on the vertical landing method to recover their booster, another promising possibility is the recovery of the first stage by horizontal landing. This method is centered around the idea to produce aerodynamic forces during re-entry to decelerate the stage and limit the aerothermodynamic loads. Thus, no additional propellant is needed and the vehicle can land horizontally on a conventional runway, however at the expense of an increase in dry mass of the system. Further, the returning stage could be captured by the innovative approach of “In-Air-Capturing”, meaning that the returning stage could be captured by a towing aircraft and pulled back to any landing site. This is currently investigated in detail in the Horizon 2020 project FALCon [3].

In the frame of defining the future technologies for reusable launch systems a multi-mission sem-reusable launch vehicle was proposed by DLR. This vehicle is capable of delivering payload of up to 14 t to GTO while having a recoverable first stage and either one or two expendable upper stages [4], [5]. Figure 1 shows a possible version of the proposed system with two expendable upper stages based on Ariane 6 heritage and a reusable first stage.

Nevertheless, the design of a winged first rocket stage capable of fulfilling its main objective, accelerating the launch vehicle from ground up to stage separation, while also being able to do an autonomous and controlled atmospheric re-

entry offers its challenges. Traversing from hypersonic to subsonic velocities, the vehicle has to be controllable at a vast range of flight conditions. Understanding the flight dynamics behind the re-entry of a winged vehicle in an early design stage is necessary to identify challenges with regards to controlling and actively steering such a high-performance vehicle in order arrive at a feasible and robust design that does not fail to converge in later design iterations. In the current preliminary design process, the focus is usually put on longitudinal trimmability and stability. However, preliminary investigations have shown that the roll and yaw movement could be highly critical to the launch vehicle design. The stage re-enters with rather high angles of attack which can cause the vertical fins to experience shadowing effects by the wings. This, in combination with a center of gravity towards the vehicle's rear, could cause potential stability issues.

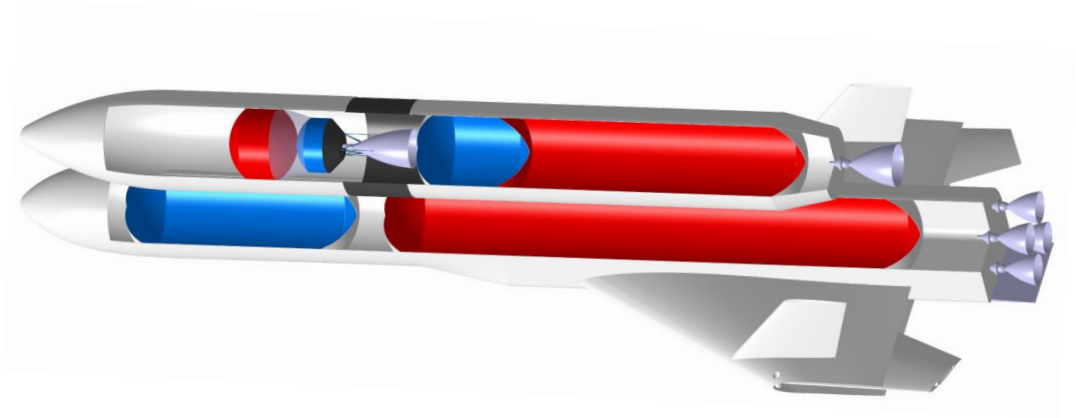

Figure 1: Multi-Mission RLV with expandable upper stages and 14 t payload to GTO

Hence, this paper focuses on analyzing the directional stability of re-entering winged stages at a preliminary stage design phase. Therefore, a first investigation is performed using the stability derivatives to determine if the current design is sufficient. Then, a linearized model was established that uses stability and dynamic aerodynamic coefficients and derivatives to determine the dynamic behavior for a linearized open-loop system. Following this, the controllability of the system is investigated by determining potential means to actively control the stage via RCS, aerodynamic control surfaces, or a mix of those. Finally, those results are used to evaluate the current design and propose potential design changes.

2. Baseline RLV Concept

The RLV stage used as baseline for the flight dynamics analysis is one of the concepts described in [5]. The first stage of the system is designed as a VTHL, which is to be captured and transported via in-air capturing after successful re-entry. The 2nd and 3rd stages are conventional ELVs based on Ariane 6 hardware. The 2nd stage features the same propellant loading (H-155) as the central stage of Ariane 6, while the 3rd stage uses the Vinci engine. The reusable first and second stages use the full-flow staged combustion engine of the SpaceLiner "SpaceLiner Main Engine", which is operated with LOX and LH2. The typical mission profile of this carrier would feature launch with ignition of the first stage engines. After main engine cut-off (MECO), the first stage would perform the aerobraking re-entry and transition to a powerless glide flight when reaching subsonic speed. At this point in flight the towing aircraft would match the stage's velocity and glide path angle to capture it in air.

The first stage of this concept was designed with different wing geometries over the course of the design definition. Double-delta wings were used as standard, and trailing edge flaps are used to control longitudinal movement. The directional control is achieved by means of two vertical fins. In addition, versions of the first stage with foldable wings were considered. These can prevent an interaction of the bow shock at the vehicle's nose with the wing's leading-edge shock which can cause highly elevated heat flux values. However, this would also result in a higher mass for the folding mechanism.

The reference concept used below is shown in Figure 2. The wing is designed as double-delta fixed wing. As aerodynamic control surfaces, a relatively large bodyflap is used, which extends over about 25% of the length of the fuselage to the end of the stage and is only used during hypersonic flight. Furthermore, elevons are used to control pitch movement, ailerons for roll control and the rudders for yaw control (see Figure 2). In addition, an RCS can optionally be used in the nose of the system for support or during exoatmospheric flight.

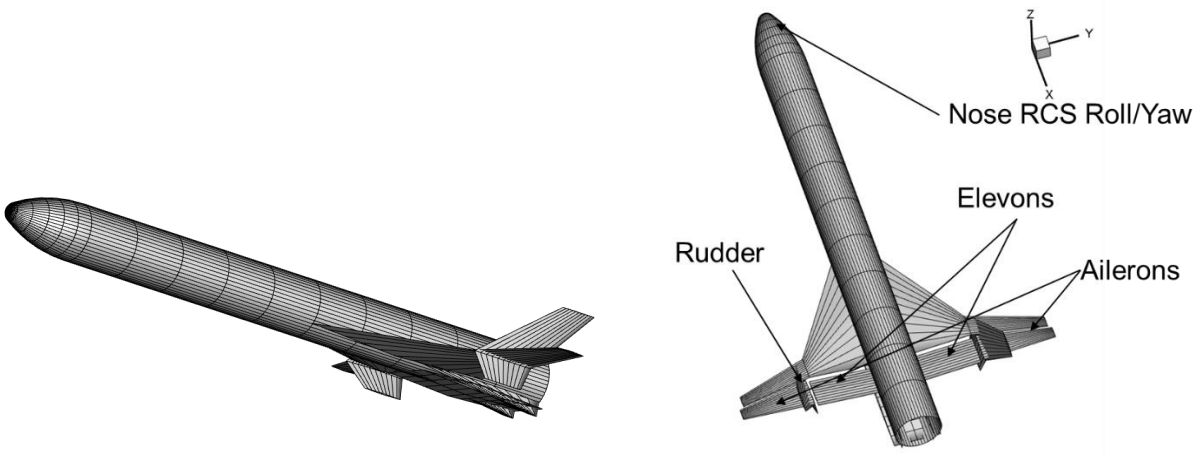

Figure 2: Geometry and control surfaces of the RLV stage

2.1 Aerodynamic Properties

The aerodynamic properties of the system were calculated with Missile DATCOM. DATCOM offers the advantage that, in addition to the usual aerodynamic coefficients such as force and moment coefficients, dynamic derivatives are also calculated. First, a trimmed aerodynamic database is created by calculating the necessary body flap and trailing (elevon) flap deflections for a torque coefficient of cm = 0 and the resulting force coefficients are obtained. The lift-to-drag ratio for trimmed conditions is shown in Figure 6 4.

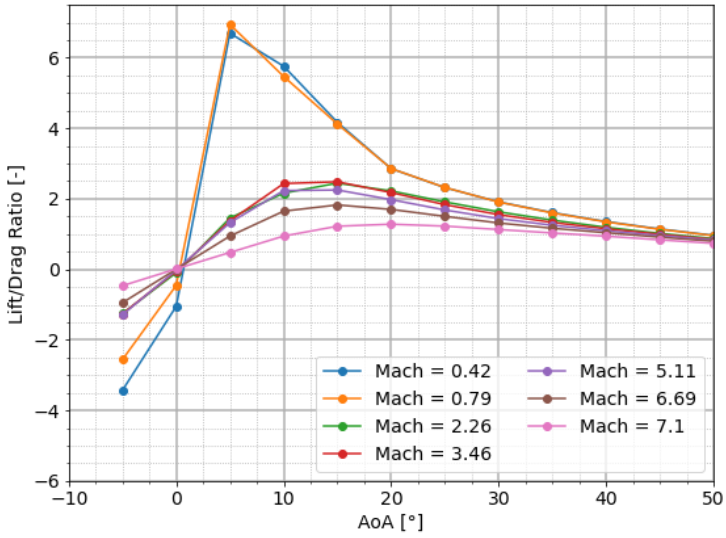

Figure 3: Lift-to-Drag Ratio of the trimmed RLV stage at different Mach numbers

2.2 Re-entry Trajectory

The re-entry trajectory of the RLV stage baseline with 3 degrees of freedom is shown in Figure 4. Following MECO, the stage coasts along a ballistic trajectory until it reaches the denser parts of the atmosphere. The AoA is kept high to produce a high amount of drag and sufficient lift to keep the stage at low-density parts of the atmosphere as long as possible in order to limit the heat flux during re-entry. The heat flux is calculated according to a simplified Fye-Ridell equation with respect to a nose radius of 1 m. Hence, the heat flux shown in the figure does not represent the maximum heat flux that is expected at parts with a small leading-edge radius, like the wing and fins leading edges.

Further, the vehicle flies several bank maneuvers in order to change the heading so that the stage flies towards the direction it is coming from when reaching subsonic speeds. Also, the bank angle is used to control the vertical amount of lift force produced. It is clearly visible in the trajectory control profile that a velocity range from subsonic (Mach = 0.4) to supersonic (Mach = 7 and more) velocities has to be covered while controlling AoAs from 0° to 40°. This

requirement is rather demanding since the aerodynamic properties of the vehicle change significantly from supersonic to subsonic velocity (see section 3).

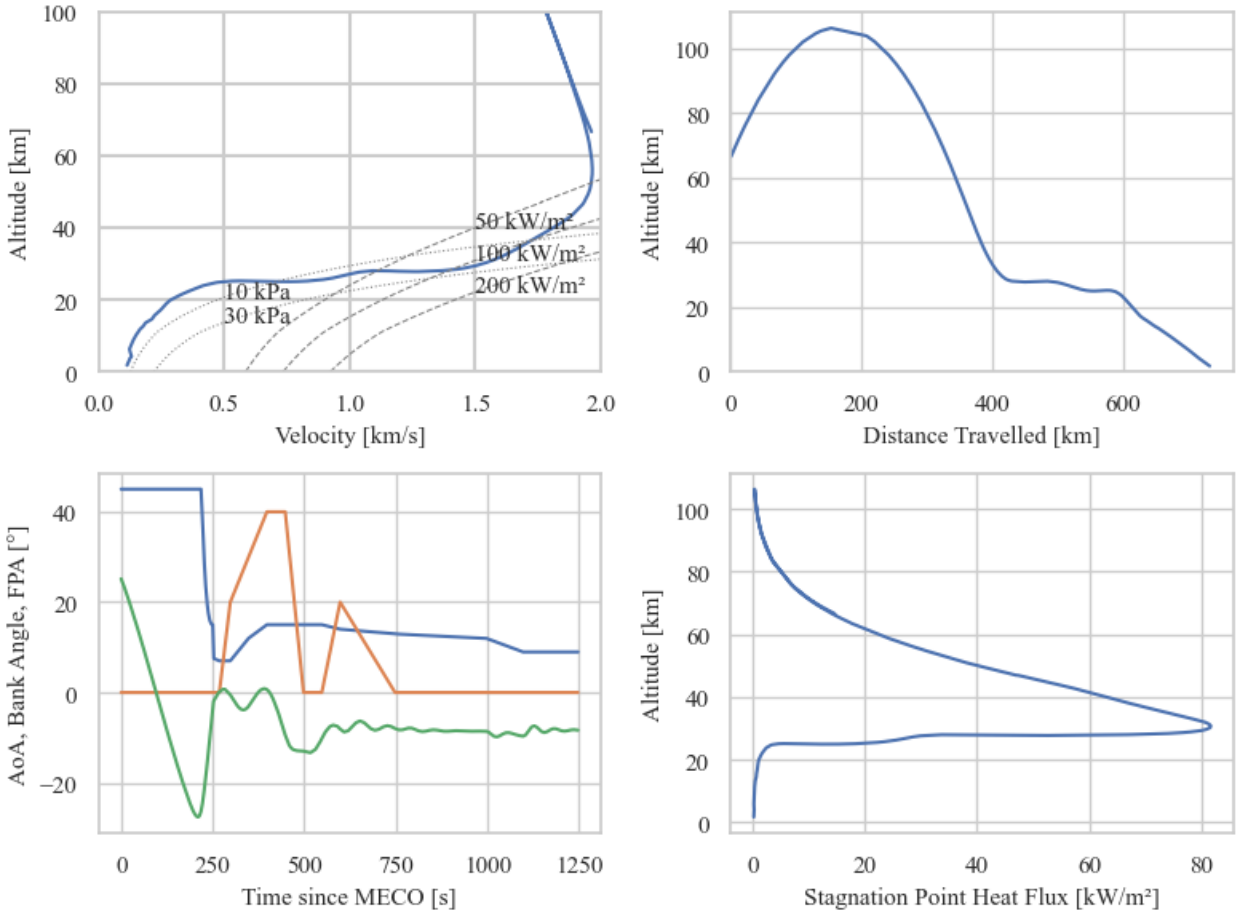

Figure 4: Re-entry Trajectory of the RLV stage

3. Stability Analysis

In the following the baseline RLV is investigated with respect to its stability and dynamic behavior. First, the longitudinal and lateral stability conditions are used to determine if the vehicle is passively stable. Then, the linearized system at specific flight points is derived to eigenvalues which can be used to assess the dynamic stability of the system.

3.1 Preliminary Analysis with Stability Criteria

According to literature the requirement for passive longitudinal stability is defined as follows [9]:

$$\frac{\Delta cm}{\Delta \alpha} \leq 0 \tag{1}$$

Here, cm is the pitching moment coefficient and α is the AoA. Figure 5 shows the values of Δcm/Δα for different AoAs and calculated along the trajectory. For most parts, the stability condition is fulfilled and the vehicle is passively stable. Instable regions are present from Mach 4.5 to Mach 5.5 and at Mach 3. Those instabilities could be avoided with a different choice of AoA in those specific regions, as stable AoAs exist. However, this could have a negative impact on the trajectory design since the required AoA in those regions has to be rather high in order to minimize heat and structural loads.

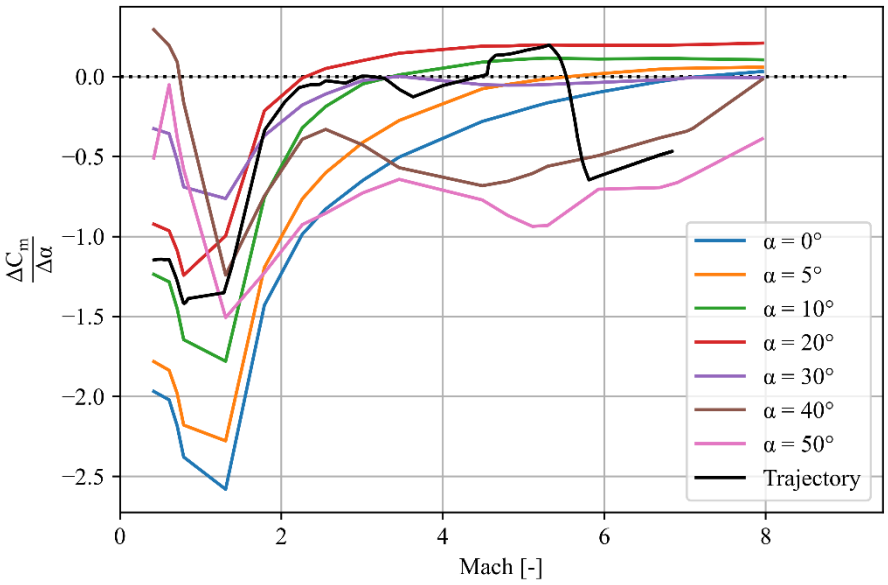

Figure 5: Change of Pitch Moment Coefficient with respect to AoA for different AoAs and along the trajectory

The criteria for directional (weathercock) static stability is defined as follows:

$$\frac{\Delta cn}{\Delta \beta} \geq 0 \tag{2}$$

Here, cn is the yawing moment coefficient and β is the angle if sideslip. Figure 6 shows the coefficient from equation (2) for different AoAs and along the whole trajectory. In this case it is clearly visible that at supersonic velocity, beyond Mach 2, the vehicle is directionally instable, since the aerodynamic center moves further downstream. In that case any disturbance would lead to an increase in disturbance which renders the vehicle unstable. Here, active control would be necessary to stabilize the vehicle. Once reaching subsonic velocity, the vehicle is directionally stable. Since this preliminary analysis has revealed problems with the directional stability, the analysis of eigenvalues was then performed in order to determine the dynamic response and also possible control means.

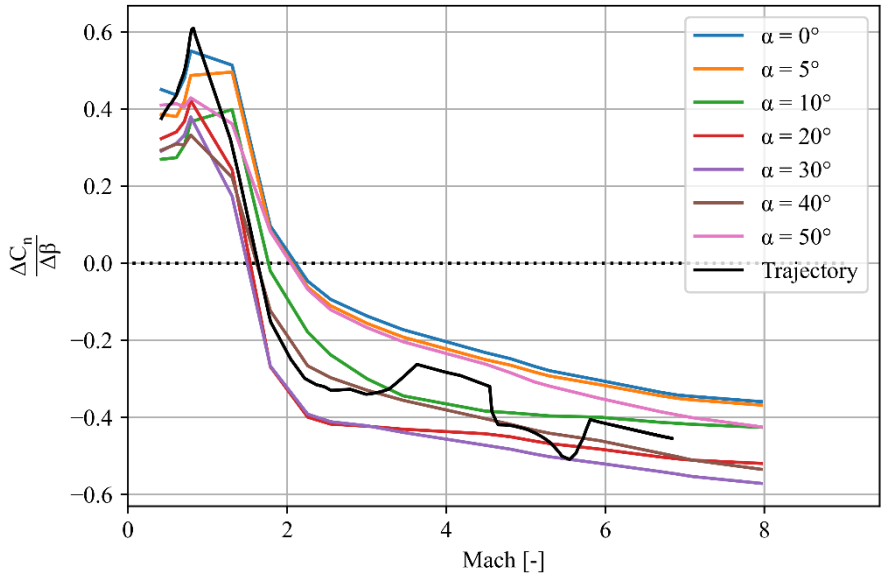

Figure 6: Change of Yaw Moment Coefficient with respect to sideslip for different AoAs and along the trajectory

3.2 Analysis of Eigenvalues

For a complete description of the flight dynamics of the RLV stage along a reference trajectory, the equations of motion with 6 degrees of freedom (6-DOF) are required. Those equations are non-linear and complex, hence a full 6-DOF

simulation requires computational effort. A simplified and faster approach to determining flight dynamics at certain flight points is the linearization of the equations of motion. This method allows to derive linear, time-invariant equations that are valid in a range of small disturbances around an equilibrium point of the vehicle (usually trim points) and are suitable for describing the flight dynamics in this area. In addition, such linearized systems can already be used to design control loops for controlling the vehicle [9], [10], [11]. The basic form of the linearized equations of motion is shown in equation (3).

$$\dot{x} = Ax + Bu \tag{3}$$

Here, x describes the vehicle's state (usually there is a distinction between the longitudinal and lateral movement), A is called the state matrix A, u is the control vector containing all information about control system deflections or impacts and the matrix B contains all information with regards to control derivatives. The state and control vectors for the RLV reference stage are, in accordance with [9], shown in equation (4). Here, u and u_∞ are axial velocity, respectively freestream velocity, θ is pitch angle, ϕ is roll angle and ψ is yaw angle.

$$x_{lon} = \begin{bmatrix} u/u_\infty \\ \alpha \\ \dot{\theta} \\ \theta \end{bmatrix}, u_{long} = \begin{bmatrix} \delta_{elevons} \\ \delta_{RCS,\,pitch} \end{bmatrix}, x_{lat} = \begin{bmatrix} \beta \\ \dot{\phi} \\ \phi \\ \dot{\psi} \end{bmatrix}, u_{lat} = \begin{bmatrix} \delta_{Ailerons} \\ \delta_{Rudder} \\ \delta_{RCS,\,roll} \\ \delta_{RCS,\,yaw} \end{bmatrix} \tag{4}$$

The complex eigenvalues of the system matrix A describe the dynamic motion of the RLV stage. By analyzing the real and complex part of each eigenvalue λ_i, the frequency ω_n of the motion (equation (5)), the damping ratio ζ (equation (6)), the period T (equation (7)) and the time to half amplitude t_{HA} (equation (8)) can be determined. Generally, the motion is stable if the real part of the eigenvalue is negative $Re(\lambda_i) \leq 0$. If $Re(\lambda_i) > 0$ then the motion is unstable, leading to a negative value for $t_{HA,}$ indicating that the amplitude actually doubles.

$$\omega_n = \sqrt{Re(\lambda_i)^2 + Im(\lambda_i)^2} \tag{5}$$

$$\zeta = \frac{-Re(\lambda_i)}{\omega_n} \tag{6}$$

$$T = \frac{2\pi}{\omega_n\sqrt{1-\zeta^2}} \tag{7}$$

$$t_{HA} = -\frac{ln2}{Re(\lambda_i)} \tag{8}$$

By checking the real and complex parts of the eigenvalues at specific points in the trajectory one can determine if the vehicle is stable or unstable throughout the flight regime. Figure 7 shows the movement of the eigenvalues throughout the trajectory. The real part of the eigenvalues is plotted along the x- axis while the imaginary part is represented on the y-axis. Eigenvalues that only have a real part are non-oscillatory movements, meaning that the respective motion is either exponentially stable or instable. Complex conjugate eigenvalues, so pairs of eigenvalues, represent oscillatory motions.

It is clearly visible that the longitudinal motion is mostly stable. Only a few eigenvalues have a real part which is in the region of Mach 5 to Mach 3 at high to medium AoA, in accordance with the analysis shown in Figure 5. Contrary to that, the lateral motion is unstable throughout most of the flight. In fact, even down to Mach 0.5 there is at least almost always one unstable eigenvalue. This observance supports the point that was already concluded by the analysis by stability derivatives, namely that the lateral motion is the more critical motion in terms of stability.

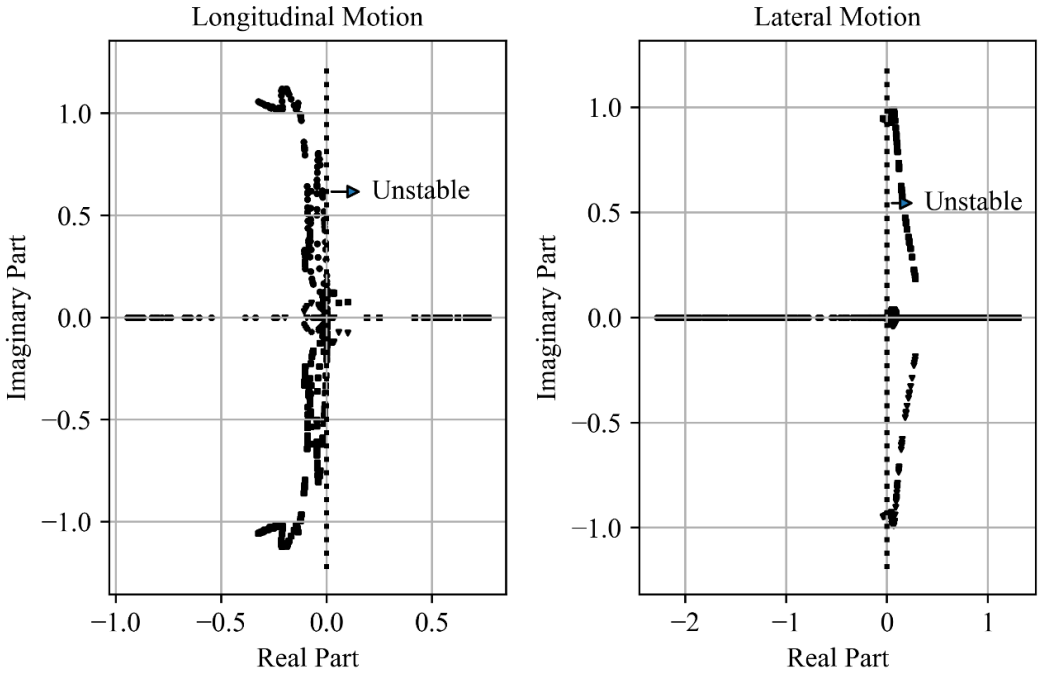

Figure 7: Eigenvalues of longitudinal and lateral motion throughout the re-entry trajectory of the RLV stage

Figure 8 and Table 1 show the eigenvalues for some selected flight points for the longitudinal and lateral motion. In both cases the vehicle is longitudinally trimmed. Two different velocities, respectively Mach = 0.4 and Mach = 5.6, were chosen to show the major difference between the dynamic behaviour at subsonic (and low AoA) and supersonic velocities (with high AoA). At subsonic velocity the typical motional modes are present. Those are a high-frequency, largely damped AoA short-period oscillation. This motion is best described by the aircraft counteracting any disturbance to the trimmed AoA (see Figure 9). Additionally, a low-frequency and only slightly damped oscillation, the phugoid, is observed. This motion is mainly described by a change in pitch angle and velocity. At supersonic velocity and high AoA, both modes are present but less damped. The critical instability in longitudinal motion is only experienced for high Mach numbers and rather low AoAs.

Table 1: Eigenvalues, period T and time to half amplitude tHA for the longitudinal motion at different flight conditions

Mach	**Aoa**	**Altitude**	**T**	**tHA**	**Mode**
0.44	12.0°	8.1 km	5.9 s	2.2 s	AoA Oscillation
			67.7 s	36.9 s	Phugoid
5.63	35°	38.5 km	9.7 s	14.9 s	AoA Oscillation
			-	40.7 s	Exp Mode 1
			-	48.9 s	Exp Mode 2

Table 2: Eigenvalues, period T and time to half amplitude tHA for the lateral motion at different flight conditions

Mach	**Aoa**	**Altitude**	**T**	**tHA**	**Mode**
0.44	12.0°	8.1 km	-	0.3 s	Roll Mode
			-	30.8 s	Spiral Mode
			6.6 s	22.1 s	Dutch Roll
5.63	35°	38.5 km	-	0.7 s	Stable Mode 1
			-	5.5 s	Stable Mode 2
			-	-0.8 s	Unstable Mode 1
			-	-40 s	Unstable Mode 2

Considering the lateral motion, the subsonic regime shows characteristic aircraft motion: a highly damped roll movement, called the roll mode (compare Table 2). Further, a low damped but also stable motion, the spiral mode and the dutch roll. The dutch roll is an oscillatory motion where sideslip and roll are constantly alternating, as shown in Figure 9). Usually, the frequency is high and the motion is not well damped. At supersonic velocities, there are two exponentially stable and two exponentially unstable modes, once again showing the need to introduce active control to the system. In fact, the critical unstable motion as shown in Table 2 has a time to double amplitude of 0.8 s (indicated by the negative sign). Here, active control is crucial to ensure a stable vehicle. Furthermore, it was observed that at subsonic velocity the spiral and roll mode are stable whereas the dutch roll movement is unstable until low Mach numbers. Hence even at such low velocities the need for active control is necessary.

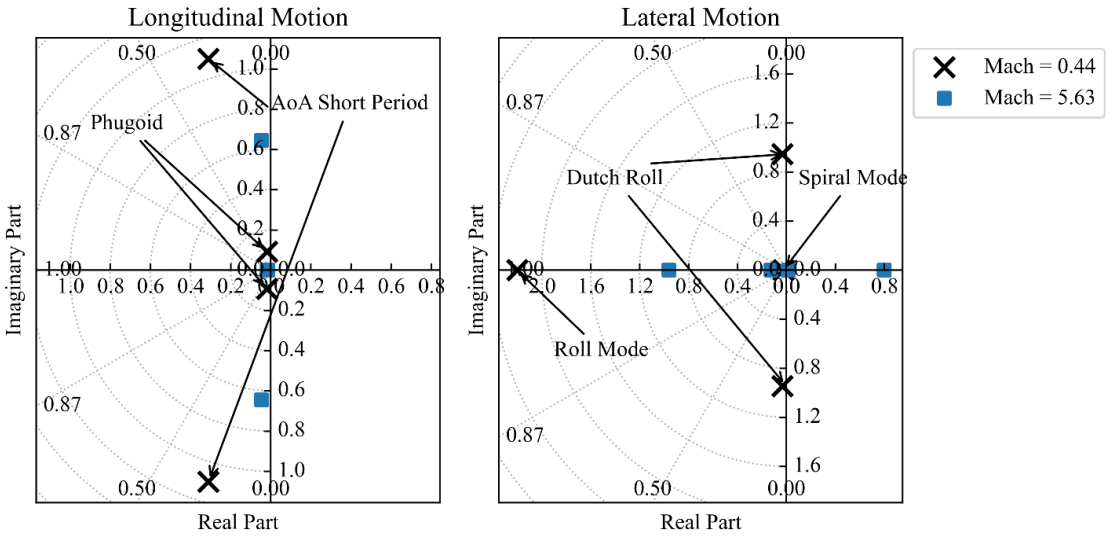

Figure 8: Eigenvalues of longitudinal and lateral motion at Mach = 0.44 and Mach = 5.63

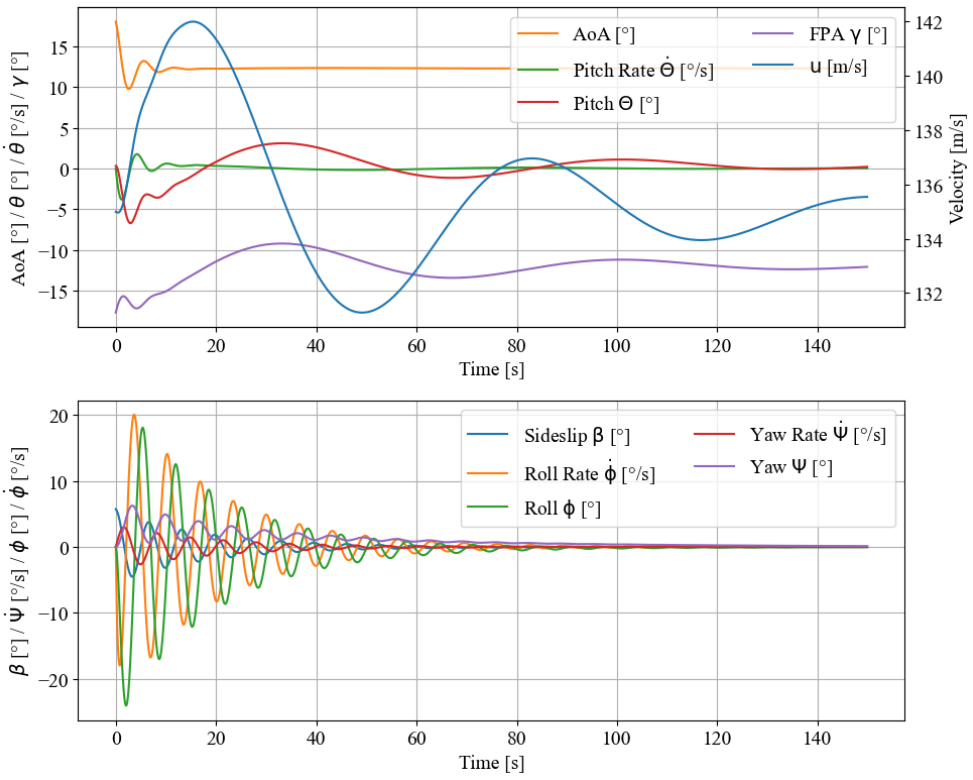

Figure 9: Dynamics of longitudinal (top) and lateral (bottom) motion of the RLV stage linearized model to disturbances in AoA (disturbance of + 5°) and β (disturbance = 5°) at Mach = 0.44

4. Closed-Loop System with active control

In this section the controllability of the vehicle shall be investigated by using state feedback. This method is depicted in Figure 10 and is based on the idea to use feedback gains K on the state of the vehicle plus forward feedback gains kf to determine control commands for the aerodynamic surfaces and RCS system. Those feedback gains can be determined by a trial and error approach or by optimization methods, such as LQR (Linear Quadratic Regulator) where state and control movement penalties have to be set to determine the control gains K.

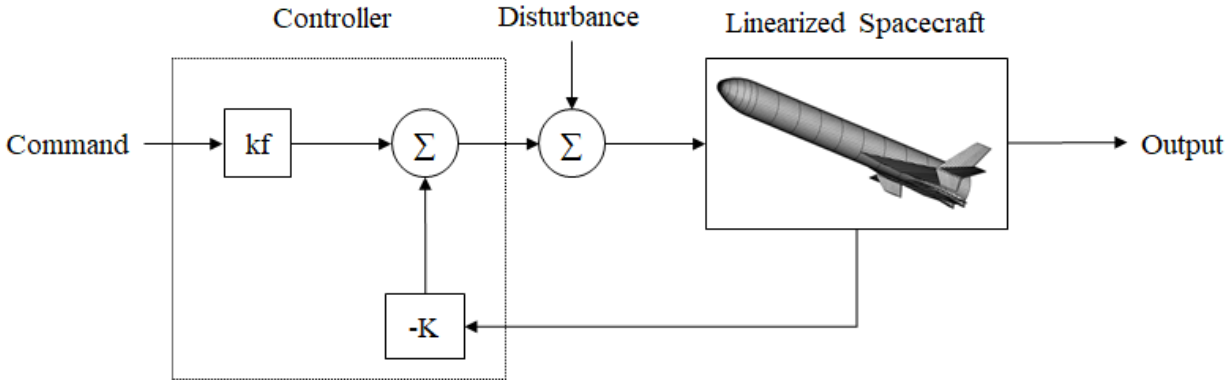

Figure 10: RLV stage controller architecture

4.1 Control with aerodynamic surfaces

The calculation of those gains is exemplary shown for the two flight points already investigated in section 3.2. As the dynamic pressure at those flight points is in the range of 4 kPa to 7 kPa only aerodynamic surfaces are used. For pitch attitude control, the elevons are used and for yaw and roll control the ailerons and rudders are used. It is important to highlight that the controller is designed on simplified assumptions, meaning infinitely fast control surfaces, no actuator model and no backlash and delay. A more detailed model should be focus of future work.

Figure 11 and Figure 12 show the eigenvalues and motions at Mach 0.44 and Mach 5.63. In both cases, the state feedback stabilizes the vehicle and all real parts of eigenvalues are negative. For longitudinal motion, the phugoid is greatly damped. In the lateral motion regime, the dutch roll is also greatly damped compared to the open loop system.

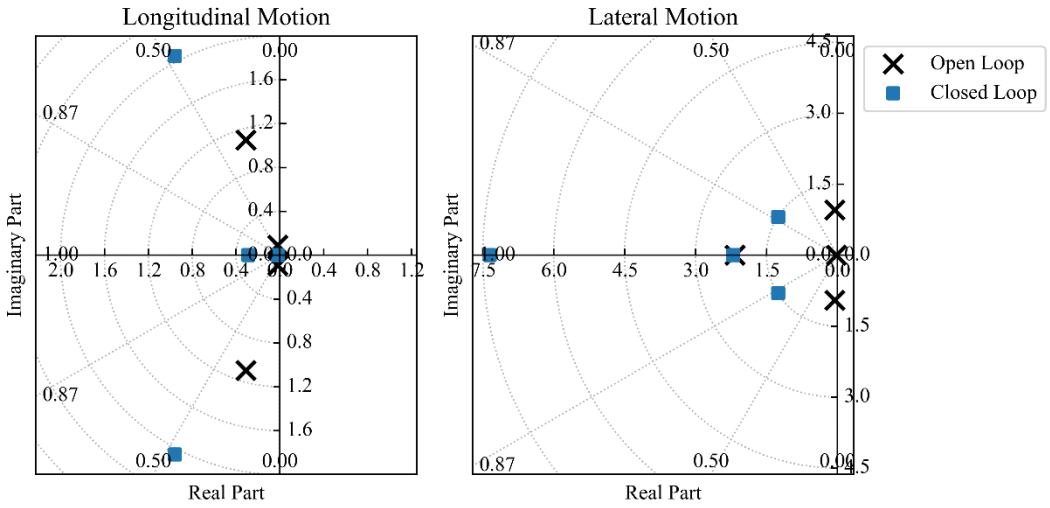

Figure 11: Open and Closed Loop Eigenvalues at Mach = 0.44

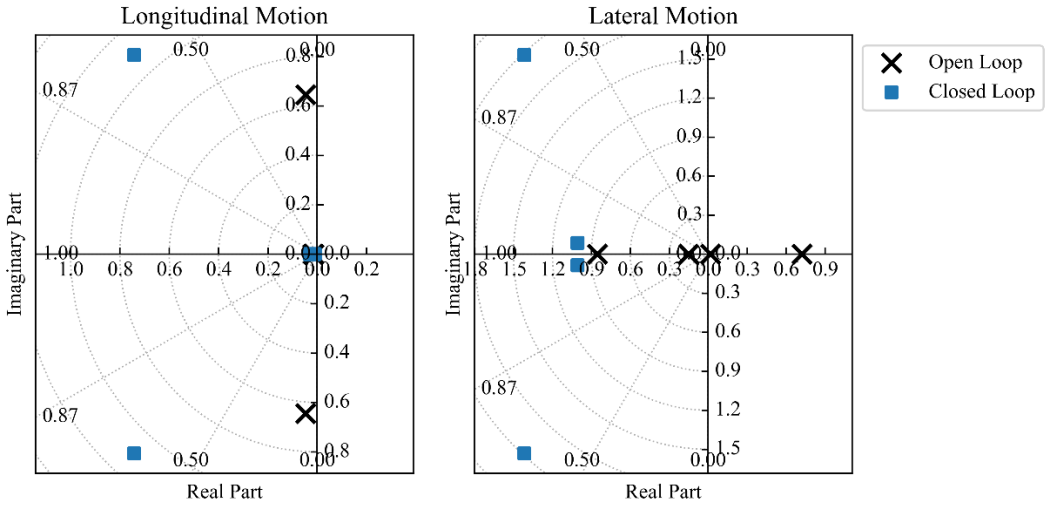

Figure 12: Open and Closed Loop Eigenvalues at Mach = 5.63

The gains calculated from the linearized state can now be used to simulate the dynamic response of the vehicle in 6-DOF. The equations of motion were taken in a simplified form from [13], assuming a flat earth and no rotation of the earth. Figure 13 shows the motion of the vehicle at subsonic velocities. The gains from the flight point at Mach = 0.44 where herein used to control the flight path angle to achieve a targeted value and control the roll angle. The simulation is initialized at v ~ 203 m/s, aoa = 5°, β = 1° and h = 10000 km, a latitude of 0° (equator) and a heading of 90°. Note that this position and initial state does not correspond to the actual values from the 3-DOF trajectory, but is set to values close to those from the trajectory. Since the goal is the demonstration of overall feasibility of the control design, this approach was deemed suitable. Further, the dotted lines in Figure 13 represent the commanded values for γ and roll angle ϕ.

Initially, the vehicle tries to reach the targeted value for γ = 12° by controlling the pitch movement via the movement of the elevons. Those are deflected to values of over -15°. Also, the initial sideslip is compensated for by simultaneous rudder and aileron deflection. After t = 62.5 s the ailerons are deflected in order to reach the targeted roll angle of ϕ = 10° and the AoA is increased in order to achieve the new γ target of -10°. The rudder is used to compensate for the induced sideslip. In total, the vehicle shows a decent controllability and dynamic response to the commanded values. Nevertheless, the controller overshoots the commanded values and tends to produce some “wobbly” behaviour for the longitudinal control, which can partly be explained by the change in roll angle commanded after 62.5 s. The change in bank angle requires a higher AoA to compensate for the reduced share of vertical lift. Here, controller fine tuning could potentially improve the whole dynamic behaviour. Nevertheless, for this work, the general feasibility to control the vehicle at subsonic speed was proven.

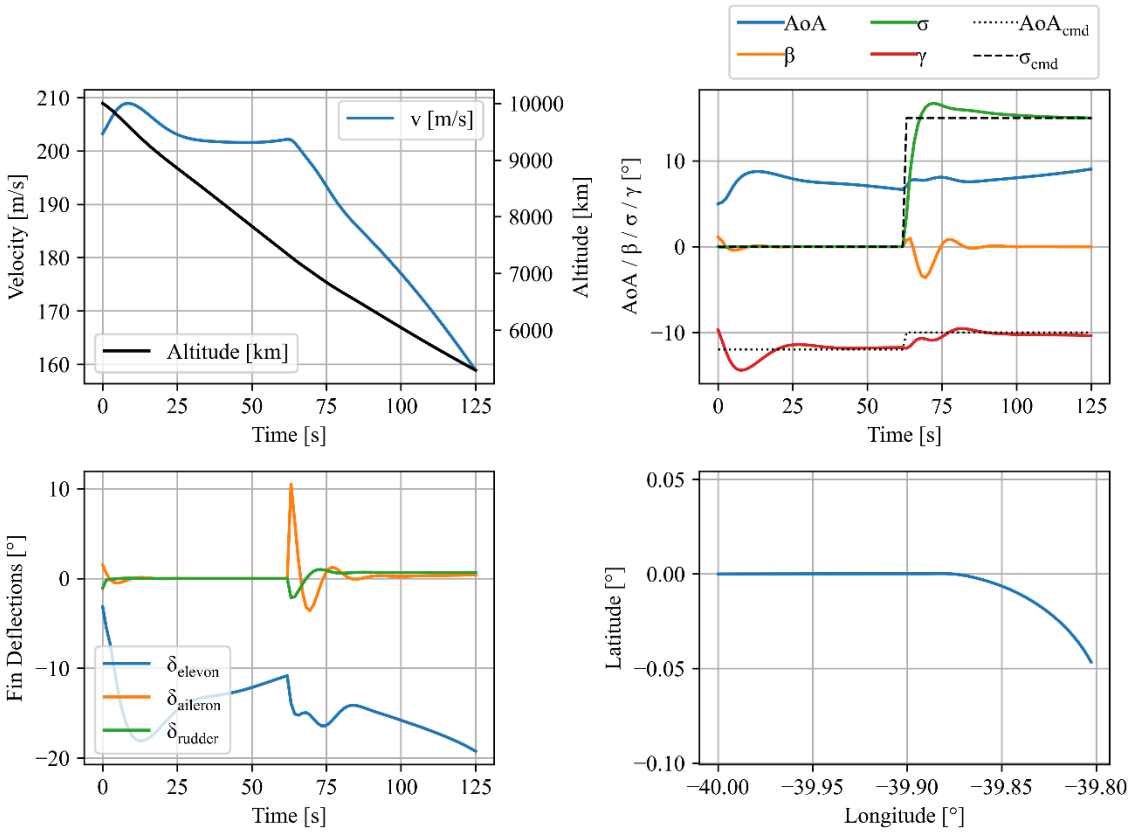

Figure 13: 6-DOF time simulation of the vehicle's closed loop motion at subsonic speed

For the time simulation at supersonic velocity a point from the 3-DOF trajectory including an AoA and bank angle profile as reference was chosen. The gains as shown in Figure 12 were used. The time simulation is initialized with a high AoA and is gradually reduced to allow almost horizontal flight. This maneuver is of high importance for the re-entry since it determines maximum heat flux and loads. As can be seen from Figure 14 the AoA and bank profile can be kept with sufficient accordance. The deviation between commanded and actual value is rather small and the trajectory resembles the 3-DOF solution from Figure 4.

Furthermore, the deflection of the elevon shows the change in aerodynamic properties along the trajectory on the one hand and the rather big range of AoAs that have to be covered. The deflection changes from almost +19° to -25°. This might be a problem since the maximum range of deflection was set to ±20° for the calculation of aerodynamic properties. Hence, the data used for the calculation of deflection derivatives is extrapolated. Nevertheless, the high deflections here indicate that the AoA profile could be adapted to allow for smaller trim deflections in the future.

The results generally show, that the re-entry trajectory can be followed and the vehicle can be actively stabilized by using a controller at the aerodynamically dominated flight phases. Nevertheless, the simulation is still rather simplified, as no actuator model, no sensor model and no state feedback model are implemented. At this preliminary design phase, the demonstration of general controllability and its limitations are of more importance and more detailed investigations would be concern of detailed work about GNC analysis and design.

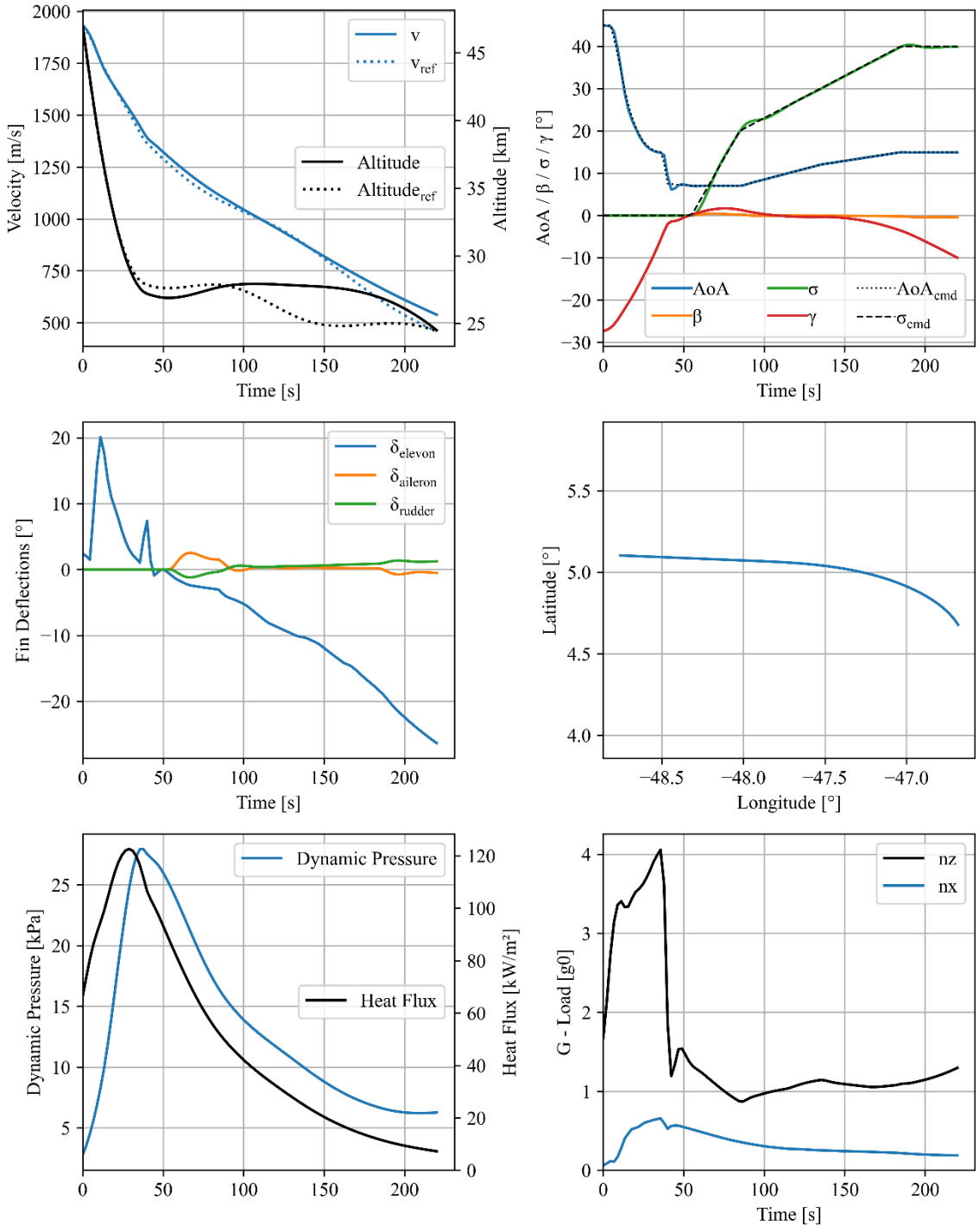

Figure 14: 6-DOF time simulation of the re-entry maneuver with closed loop

4.2 Control with RCS

In the previous section the controllability of the vehicle by using the aerodynamic surfaces was investigated. Nevertheless, the vehicle travels through very thin layers of the atmosphere and thus experiences conditions with almost no aerodynamic interaction through its flight. Hence, controllability of the vehicle by using the reaction control system is a further point to be investigated and demonstrated.

For this purpose, the RCS is foreseen to be installed in the vehicle's nose. The RCS should provide independent control of each axis, meaning roll, pitch and yaw. For each axis, 4 RCS engines are foreseen, with a vacuum Isp of 250 s and

a thrust of 650 N each. The distance to the CoG is estimated at 30 m along the x-axis. The minimum impulse duration of one RCS pulse is set to t = 0.2 s

For this paper, only the controllability in the exoatmospheric flight phase of the system was modelled. Therefore, the linearized system as discussed in section 3 was determined and control is established via RCS only, without using additional aerodynamic surfaces. Further, the dynamic response of the system is shown for the linearized state only, since the 6-DOF simulations for the discrete model of the RCS thrusters is challenging and foreseen for future work.. Furthermore, another interesting analysis would be to simulate the re-entry with a mix of RCS and aerodynamic surface control to determine when the RCS can be shut down. This analysis is also foreseen for future work.

Similar to the procedure described for the control with aerodynamic surfaces, the system gains K are determined in order to establish a stable closed-loop system with full-state feedback. The vehicle is initialized at a velocity of v = 1756 m/s or 6.5 and an altitude of h = 105 km. The initial AoA is disturbed by 0.15 rad (~8.6°) after t = 5 seconds into the simulation, β and ϕ are disturbed by 0.1 rad (=5.72°). Figure 15 and Figure 16 show the respective dynamic response to those disturbances. As for the longitudinal motion, the RCS engines fire instantly. Initially, 2 engines counteract the pitching moment with one engine being subsequently shut off. Once the original AoA is reached again, the pitch RCS continues to keep the new attitude with small firings of the thrusters every once in a while. Note that the RCS control pulse values can only be a natural number since each engine can be either on or off and up to 4 engines can fire simultaneously.

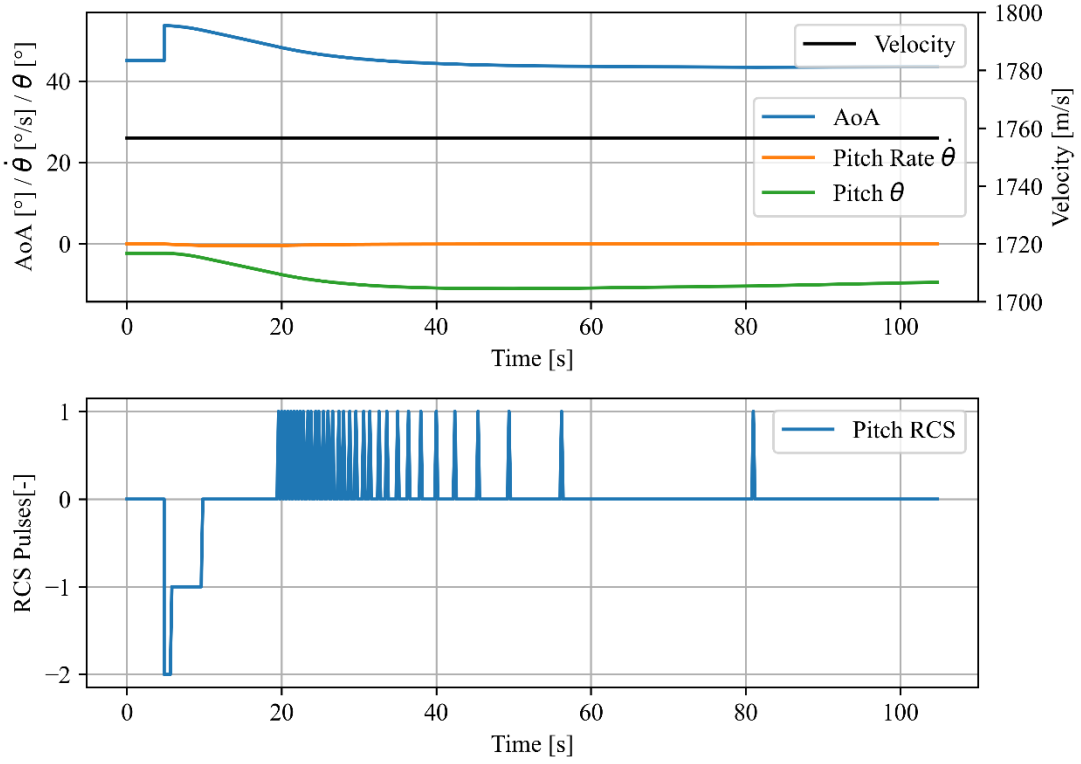

Figure 15: Longitudinal motion with RCS control to a disturbance in AoA

Considering the later response, both yaw and roll RCS start firing for some seconds to counteract the motion set into play. Once the new attitude is reached, the RCS pulses every once in a while, comparable to the pitch control. This control behaviour is called a hysteresis control, where the desired attitude is reached and controlled within certain boundaries. Those boundaries can be set quite narrow, which results in higher propellant use, or wider, which needs less propellant but the control is not as tight. The Space Shuttle Orbiter also had two different levels of control for the RCS, one for very fine maneuvering and one for faster but not as precise maneuvers. How to design the RCS control is a question of GNC design and desired controllability. Nevertheless, as for the aerodynamic control, the purpose for this paper is to prove the general controllability of the vehicle in exoatmospheric flight and at aerodynamically-dominated flight. This can definitely be validated by the simulations herein. Nevertheless, future work should focus on studying different possibilities for RCS design and interaction with aerodynamic surfaces.

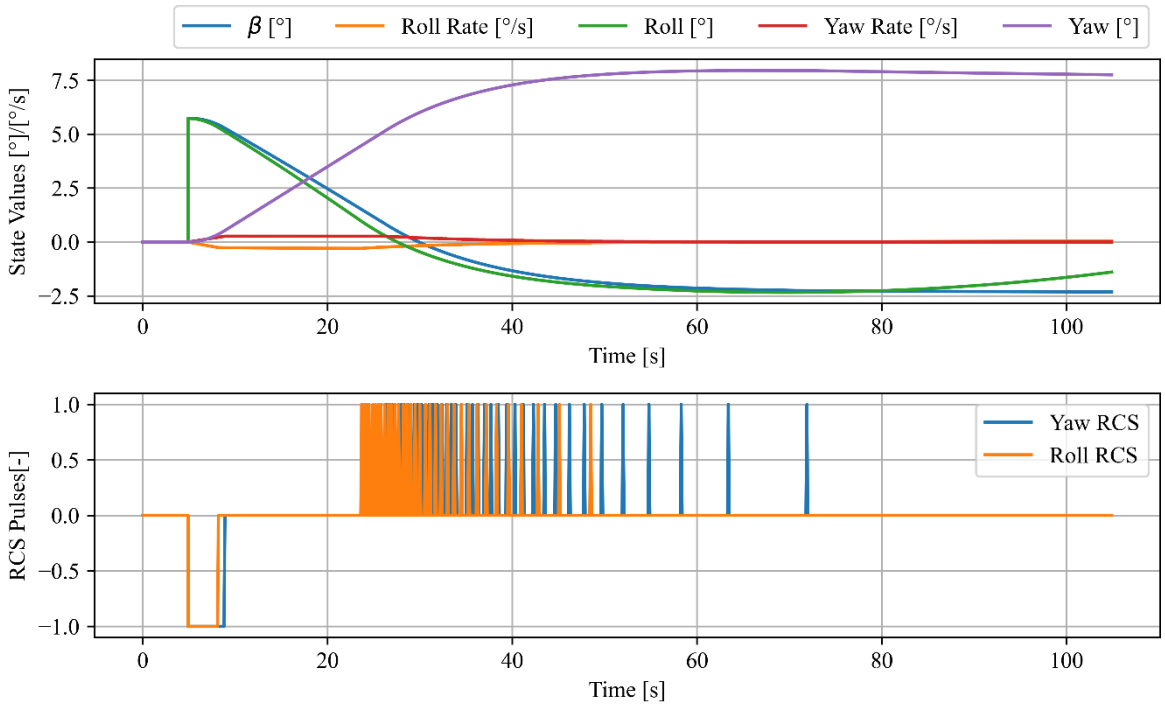

Figure 16: Lateral motion with RCS control to a disturbance in β and roll ϕ

5. Summary & Outlook

In this paper a winged reusable first stage was investigated in terms of flight dynamics, control and stability. Since a winged stage returning from suborbital velocity covers a vast range of different flight conditions, it is important to understand the flight behavior of such a system in order to identify challenges and possible showstoppers.

Therefore, an aerodynamic database was created including aerodynamic and control derivatives. Using conventional methods to assess the stability of the vehicle, such as the slope of the moment coefficient with change of angle of attack, potential instabilities at hypersonic velocities could already be observed, especially for lateral stability. Using linearized flight dynamics, the eigenvalues and motions of the RLV stage could be determined in more detail, including also the investigation of dynamic stability. Thus, it could be observed that the lateral instability is rather bad in terms of time to double the amplitude of disturbances, which is less than a second for the worst cases. It could thus be concluded that the current design of the vehicle does not allow for passive stabilization through the entire trajectory.

Looking into the possibility to actively control the stage at aerodynamically-dominated flight points, the linearized system was used to determine the gains of a preliminary, simplified control system. Thus, the closed-loop dynamic behavior of the system could be investigated. Using active control, the vehicle can be kept stable longitudinally and laterally while following the reference control profiles in a 6-DOF simulation. Nevertheless, the assumptions used for modelling the control system are rather simplified with immediate responding actuators, perfect and complete state feedback and no sensor models in the loop. However, at this preliminary design phase those questions are not of major interest and are to be answered in more detailed analysis in possible future work.

For flight outside of the atmosphere at low dynamic pressure, the possibility to control the system with an RCS was investigated. Again, the general controllability with such a system could be proven, however, only for linearized dynamics yet. The simulation of such a system for full 6-DOF is topic of future work. Also, the possibility to control the system by a mix of RCS and aerodynamic control surfaces should be investigated.

Nevertheless, an analysis routine to investigate the flight dynamics of winged stage at an early, preliminary, design phase could be established. This routine can be further used to investigate flight dynamics of winged stages and establish control systems if necessary. Future work will also focus on applying the herein described method to other vehicles.

References

[1] Stappert, S., Madalin, S., Sippel, M.: Technical Report on different RLV return modes' performances, D2.1, FALCon project deliverable, 2020

[2] Stappert, S., Sippel, M., Bussler, L., Wilken, J. : Return Options, AKIRA Bericht R-2003, 2019

[3] Sippel, M., Stappert, S., Bussler, L., Krause, S., Cain, S., Espuch, J., Buckingham, S., Penev, V.: Highly Efficient RLV-Return Mode "In-Air-Capturing" Progressing by Preparation of Subscale Flight Tests. 8TH EUROPEAN CONFERENCE FOR AERONAUTICS AND SPACE SCIENCES (EUCASS) 2019, 01.-04. Juli 2019, Madrid, Spanien.

[4] Sippel, M., et al.: A viable and sustainable European path into space – for cargo and astronauts. In: Proceedings of the International Astronautical Congress, IAC. 72nd International Astronautical Congress (IAC), 25.-29.10.2021, Dubai. ISSN 0074-1795.

[5] Callsen, S., Stappert, S., Sippel, M.: Study on Future European Winged Reusable Stages, 9th European Conference for Aeronautics and Space Sciences (EUCASS), 26th June – 1st July 2022, Lille, France

[6] Stappert, S., Sippel, M., Bussler, L., Wilken, J.: Return Options, AKIRA Bericht R-2003, 2019

[7] Stappert, S., Wilken, J., Bussler, L., Sippel, M., Karl, S. Klevanski, J., Hantz, C. und Briese, L.E., Schnepper, K.: European Next Reusable Ariane (ENTRAIN): A Multidisciplinary Study on a VTVL and a VTHL Booster Stage. In: Proceedings of the International Astronautical Congress, IAC. 70th International Astronautical Congress, 21.10-25.10.2019, Washington DC

[8] Stappert, S., Wilken, J., Bussler, L., Sippel, M.: A Systematic Comparison of Reusable First Stage Return Options. 8TH European Conference For Aeronautics and Space Sciences, 01.07.2019 - 04.07.2019, Madrid

[9] Etkin, B., Reid, L.D.: Dynamics of Flight Stability and Control, 3rd Edition, 1996

[10] Stevens, Brian L., et al.: Aircraft Control and Simulation: Dynamics, Controls Design, and Autonomous Systems, John Wiley & Sons, Incorporated, 2015.

[11] Schmidt, Louis V.: Introduction to Aircraft Flight Dynamics, American Institute of Aeronautics and Astronautics, 1998.

[12] Sippel, M., Stappert, S., Bussler, L., Krause, S., Cain, S., Espuch, J., Buckingham, S., Penev, V.: Highly Efficient RLV-Return Mode "In-Air-Capturing" Progressing by Preparation of Subscale Flight Tests. 8TH EUROPEAN CONFERENCE FOR AERONAUTICS AND SPACE SCIENCES (EUCASS) 2019, 01.-04. Juli 2019, Madrid, Spanien.

[13] Mooij, E.: Characteristic Motion of Re-entry Vehicles, AiAA Atmospheric Flight Mechanics Conference, 2013, Boston, Massachusetts, USA, https://doi.org/10.2514/6.2013-4603